Results and Discussion

4.0 RESULT AND DISCUSSION

Nanotechnology is a rapidly growing multidisciplinary field which includes many branches of science like physics, material sciences, biotechnology, super molecular chemistry, chemical engineering, mechanical engineering and medicine (Donda *et al.*, 2013). Nanotechnology manipulates matters and creates new nanoproducts with novel properties at an atomic scale (Ciobanu *et al.*, 2013). In the modern field of material science nanotechnology is one of the upcoming areas of research (Geoprincy *et al.*, 2013).

Medicinal plants represent a rich source of antimicrobial agents. Plants have a great potential for producing great benefit to mankind. There are many approaches to search for biologically active principles in plants (Malar *et al.*, 2011).

Medicinal plants are nature's gift to cure limitless number of diseases among human beings. The abundance of plants on the earth's surface has led to an increasing interest in the investigation of different extracts obtained from traditional medicinal plants as potential sources of new antimicrobial agents (Bushra and Ganga, 2011). The medicinal value of plants lies in some chemical substances that produce a definite physiological action on the human body. The most important of these bioactive compounds of plants are flavonoids, alkaloids, phenolic compounds and tannins (Edeoga, 2011).

In this study, the methanolic extract of *A. adenophora* leaves were used to prepare silver nanoparticles. The study was formulated to optimize and compare the methods of synthesis of silver nanoparticles from the methanolic extract of *A. adenophora* leaves and we analyzed the antimicrobial activity against clinical isolates. Among the bacterial strains, *Staphylococcus aureus*, *Salmonella typhi*, *Pseudomonas aeruginosa*, *Escherichia coli*, *Shigella flexneri*, *Klebsiella pneumoniae* and *Proteus vulgaris* were used and among the fungal strains *Aspergillus niger*, *Aspergillus flavus*, *Aspergillus fumigatus*, *Candida albicans*, *Rhizopus indicus* and *Mucor oryzae* were used. The efficacy of eupalitin to dock with the target protein dihydrofolate reductase of different microorganism namely *Staphylococcus aureus*, *Escherichia coli*, *Bacillus anthracis*, *Candida glabrata* and *Candida albicans* has been determined. The results obtained are presented and discussed below.

Visible color change of AgNPs

The silver nanoparticles were synthesized using four different methods, namely heating in water bath (60°C), microwave heating, room temperature and exposure to sunlight. The synthesis of nanoparticles was noticed by a change in color and the increase in absorbance. As per the results of the study, all the four methods, namely heating in water bath (60°C), microwave heating, room temperature and exposure to sunlight were efficient in the synthesis of AgNPs. But, there were some difference in the pattern of synthesis of particles between each method.

The silver nanoparticles (AgNPs) synthesized on exposure to sunlight for 20 minutes showed the maximum yield and efficiency after 24 hrs. From the visual color change we can get preliminary information regarding the formation of silver nanoparticles. As the silver nanoparticles are formed, the color of the solution changes from pale green to brown which is an indication of the presence of silver nanoparticles. The variation of the color was due to the change in surface plasmon resonance of silver nanoparticles during the formation.

PLATE 2

Visible colour change during the formation of AgNPs

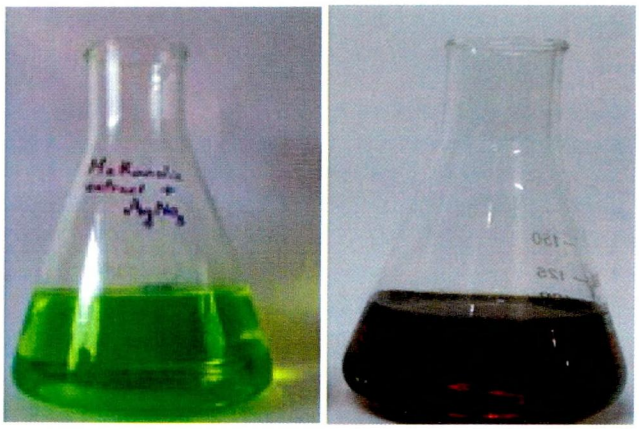

The fresh suspension of *E. Chapmaniana* was initially yellow in colour and after addition of $AgNO_3$ and exposure to bright sunlight, the suspension turned reddish brown (Sulaiman *et al.,* 2013). Khan *et al.* (2013) reported that the addition of *P. glutinosa* plant extract into the aqueous solution of $AgNO_3$, the color of the solution gradually changed from light yellow to brown, which indicates the formation of Ag NPs. Silver nanoparticles exhibited dark reddish-brown

color in aqueous solution due to the surface plasmon resonance phenomenon. Reduction of silver ion into silver nanoparticles during exposure to the plant extracts could be followed by color change (Krishnaraj *et al.*, 2010). According to the work of Augustine *et al.* (2013), the silver nanoparticles are formed, as the color of the solution changes from white to pale yellow to brick red which is an indication of the presence of silver nanoparticles. The variation of the color was due to the change in surface plasmon resonance of silver nanoparticle during the formation.

CHARACTERIZATION OF SILVER NANOPARTICLES

The synthesized silver nanoparticles were characterized as per the methods explained below.

UV-VISIBLE SPECTROSCOPY

Ultraviolet-visible spectrometry was used to examine the size and shape of the nanoparticles in aqueous suspension. The synthesized silver nanoparticles mediated by *A. adenophora* leaf extract were subjected to optical measurements by UV-visible spectroscopy, showed absorbance peaks within the range 400-450 nm which indicates the presence of silver nanoparticle.

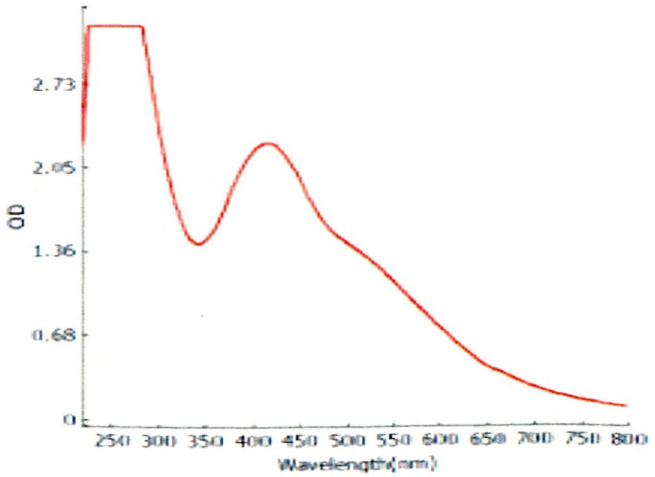

FIGURE 2

Extinction spectrum of AgNPs synthesized from *A. adenophora* leaves during exposure to sunlight for 20 minutes

The production of the silver nanoparticles synthesized from the *E. chapmaniana* leaf extract was evaluated through spectrophotometry at a wavelength range of 350-700 nm which revealed a characteristic peak at 413 nm for *E. chapmaniana* AgNPs, which confirmed the formation of the silver nanoparticles (Sulaiman *et al.*, 2013). Depending upon the shape and size of the NPs, AgNPs exhibit absorption under a visible range of 380–450 nm (Kumar *et al.*, 2012). Dubey *et al.* (2009) have reported that the silver surface plasmon resonance band occurs at 412 nm and steadily increases in intensity as a function of time of reaction is observed in the UV-visible spectra recorded from the aqueous silver nitrate and *Eucalyptus hybrida* leaf extract.

Bioreduction of Ag to AgNPs mediated by *D. bulbifera* tuber extract was examined by recording the absorption spectra as a function of time with an absorbance maximum at 450 nm, the yellowish-brown color of silver nanoparticles arises due to excitation of surface Plasmon vibrations (Ghosh *et al.*, 2012). Karunakar *et al.* (2013) reported that the UV spectral analysis gave maximum absorption spectra within the range of 450nm-470nm both for *Phyllanthus reticulatus* leaf and root mediated particles which stands as a strong proof to report them as silver nanoparticles.

Formation of stable silver nanoparticles using the seed extract of *Jatropa curcas*in aqueous colloidal solution were confirmed using UV– visible spectral analysis with a characteristic SPR at 425nm (Bar *et al.*, 2009).

With reference to the above literature, it is evident that the characteristic increase in absorption in the range of 400- 450nm confirmed the synthesis of silver nanoparticles from *A. adenophora* leaf extract.

SCANNING ELECTRON MICROSCOPY (SEM) - EDAX SPECTRA

Scanning Electron Microscopic studies were carried out to study the morphology of the silver nanoparticles. It is evident that the AgNPs were roughly spherical in shape. The average size was around 100nm for the AgNPs synthesized from methanolic extract of *A. adenophora* leaf extract. EDAX analysis confirmed the presence of the element silver as the major constituent.

The SEM image showing the high density Ag-NPs synthesized by the *Gelidiella acerosa* confirmed the development of silver nanostructures. The SEM micrographs of silver nanoparticle

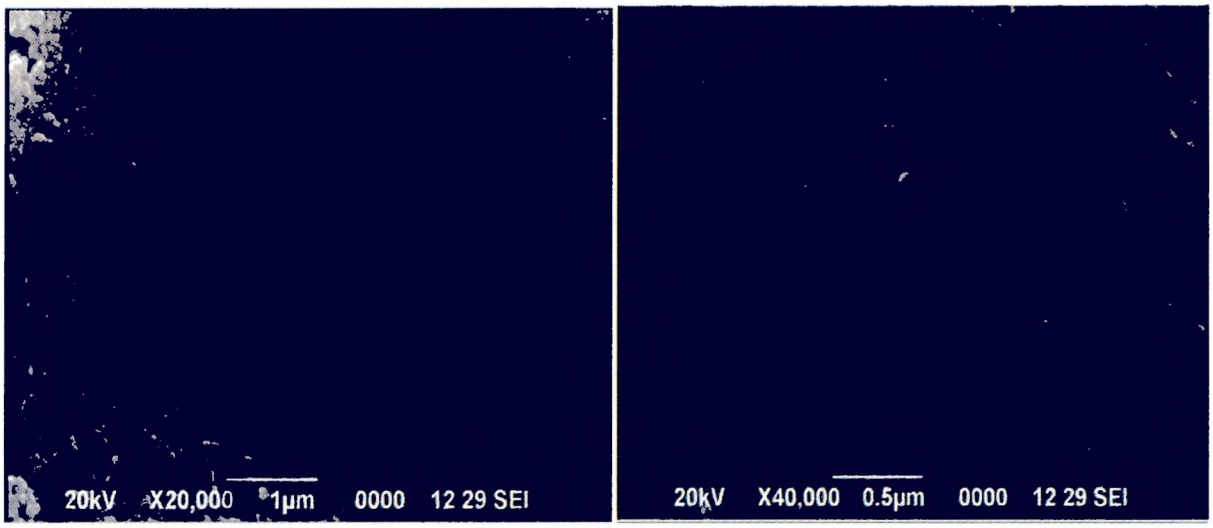

PLATE 3

SEM image of synthesized silver nanoparticles

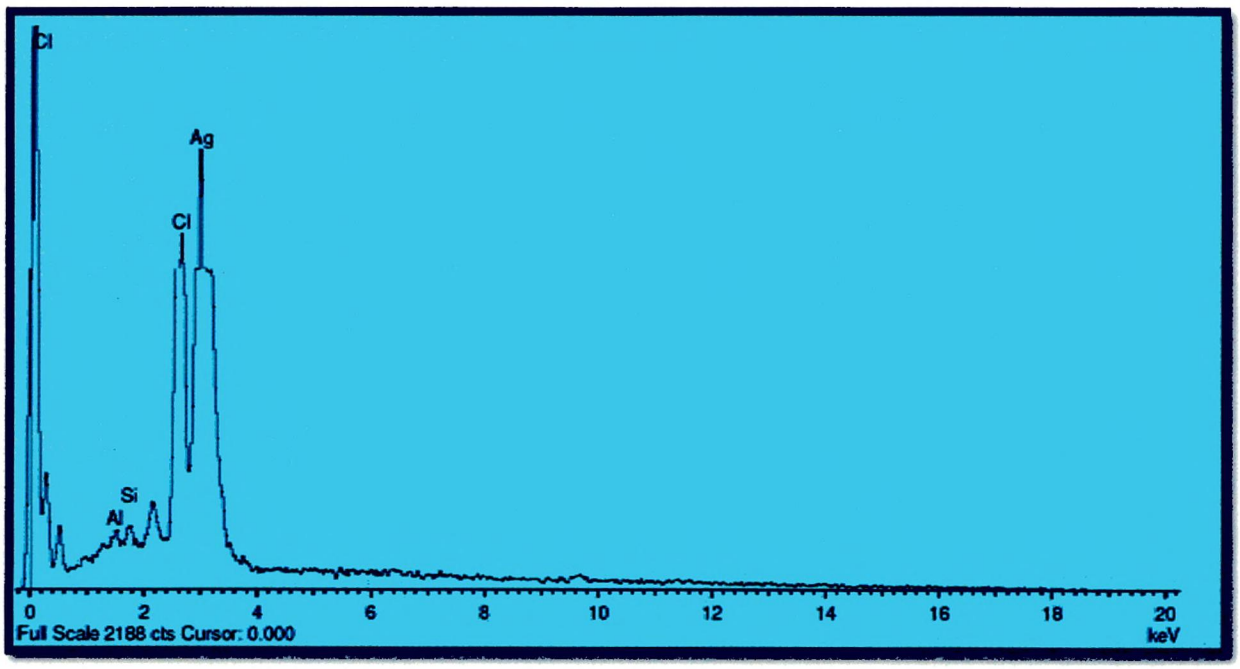

FIGURE 3

EDAX profile of synthesized silver nanoparticles.

obtained in the filtrate showed that Ag-NPs are spherical in shape, which is well distributed without aggregation in solution (Vivek *et al.*, 2011).

The silver nanoparticles synthesized from piper nigrum fruit extract were predominantly spherical with uniform shape. The SEM image exposed that the formed nanoparticles were within the size range of 40- 60nm (Mani *et al.*, 2012). The SEM results indicated that the AgNPs formed from *Securinega leucopyrus* were from spherical to oval in shape with a smooth morphology.The element silver is confirmed as the major constituent from EDAX analysis (Donda *et al.*, 2013).

According to the work of Shameli *et al.* (2012) the exterior surfaces of Ag/*C. longa* due to the presence of Ag-NPs become shiny in the spots' spherical shapes. The EDXRF spectra for the *C. longa*, the peaks around 1.3 to 3.4 keV were related to the silver elements. These results confirm that the extract can effectively control the shape and size of the Ag-NPs.

Pavani *et al.* (2013) explained that AgNPs synthesized from *Ipomoea indica* flower extract were cuboid and spherical in shape, with a size range 5-50nm

The formation of silver nanoparticles as well as their morphological dimensions in the SEM study demonstrated that the average size was from 35-55 nm with inter-particle distance. The shapes of the silver nanoparticles synthesized from *Catharanthus roseus* are proved to be spherical. From EDX spectra it is proved that AgNPs reduced by *C. roseus* has the weight percentage of the element silver as 20.16 and 16.41 (Ponarulselvam *et al.*, 2011).

FOURIER TRANSFORM INFRARED (FTIR) SPECTROSCOPY

The FTIR measurements of biosynthesized silver nanoparticles were carried out to identify the possible interaction between protein and silver nanoparticles. The FTIR analysis was carried out to find out the capping material (i.e the possible functional groups involved) present in the particles which enable the synthesis. The FTIR spectra of leaf extract mediated silver nanoparticle showed peaks indicating prominent absorption at 2924 cm^{-1}, 2301 cm^{-1}, 1516 cm^{1},1383 cm^{-1}, 1070$cm^{-1}$and 678 cm^{-1}.

The result indicates that the carboxyl (-C =O), hydroxyl (-OH), and amine (-NH) groups are mainly involved in the synthesis of silver nanoparticles. These groups which are commonly

found in the proteins indicate that the presence of proteins as capping agents for silver nanoparticles increase the stability of the nanoparticle synthesis. Minor peaks indicate that the formed silver nanoparticles were surrounded by proteins, terpenoids and other secondary metabolites.

Kora *et al.* (2012) reported that both hydroxyl and carboxyl groups of gum are involved in the synthesis of silver nanoparticles. Phenolic compounds and saponins present in plants extract bind to nanoparticles via either free amine groups or cystein residues in protein (Shankar *et al*, 2003).

FIGURE 4

FTIR spectra of silver nanoparticles

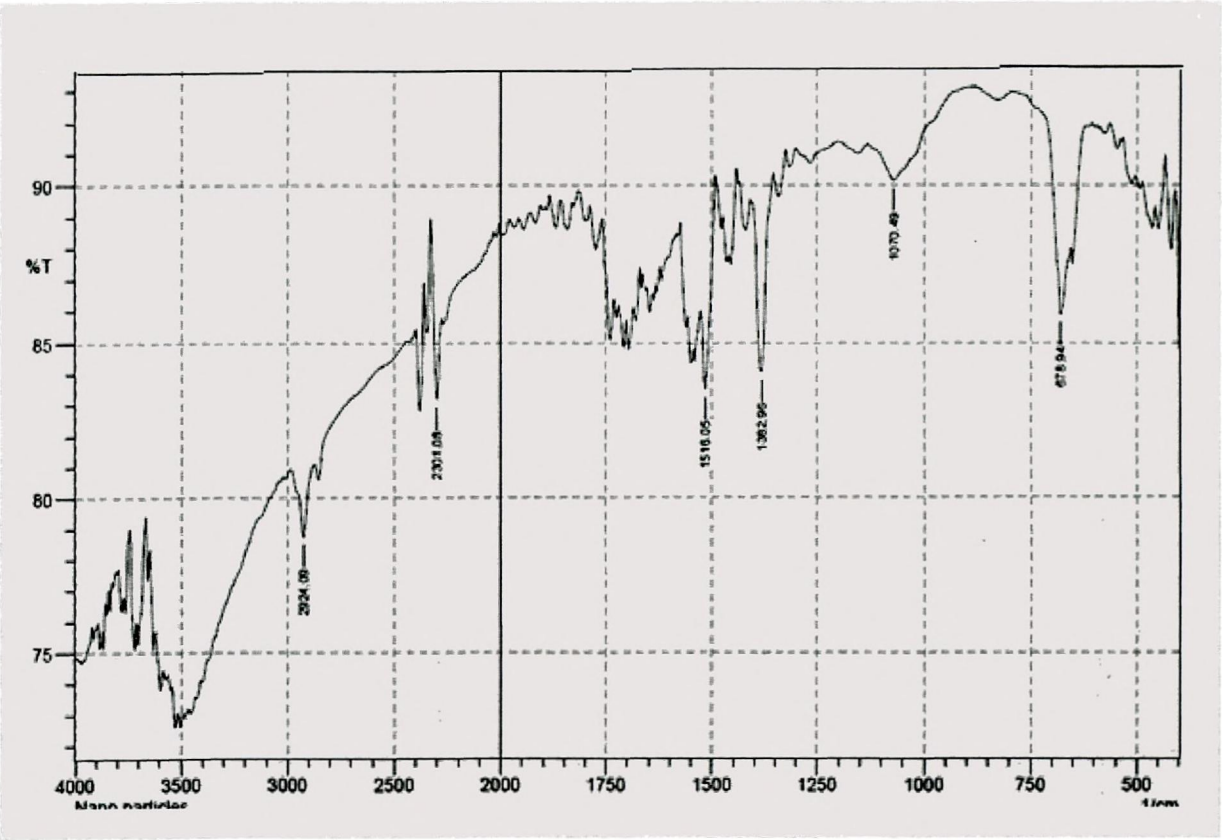

The *M. umbellatum* proteins adsorb as a layer over the green-synthesized silver nanoparticles, which stabilizes them. Proteins can bind to silver and gold nanoparticles via either free amine groups or cysteine residues in the phenolic compounds, quinones and saponins from

M. umbellatum, which stabilize the nanoparticles formed through the surface-bound proteins (Arunachalam *et al.*, 2013).

Further, Donda *et al.* (2013) suggested that the Carboxyl (-C=O), hydroxyl (-OH) and Amine (-NH) groups of *Securinega leucopyrus* leaf extracts are mainly involved in synthesis of silver nanoparticles. Other minor peaks indicate that the formed silver nanoparticles were surrounded by proteins, terpenoids and other secondary metabolites.

The observed peaks of *M. edule* are more characteristic of flavonoid and terpenoid group components in having the ability to absorb on the surface of silver nanoparticles. It plays a major role in the reduction of nanoparticles by interaction through carbonyl groups and in the oxidation of aldehyde groups in carboxylic acids (Elavazhagan and Arunachalam, 2011).

FTIR analysis reveals that the biological molecules present in the sample could possibly have the functional groups which facilitate the formation of silver nanoparticles. Thus, all the physicochemical characteristics (UV-absorption spectrum, SEM imaging and FTIR analysis) in the present study confirmed the nature of the silver nanoparticles synthesised from *A. adenophora* leaf extract.

ANTIMICROBIAL ACTIVITY

In this study, we analyzed the antimicrobial activity of silver nanoparticles synthesized from *A. adenophora* leaf extract against clinical isolates. Among the bacterial strains, *Staphylococcus aureus*, *Escherichia coli*, *Pseudomonas aeruginosa*, *Salmonella typhi*, *Klebsiella pneumonia, Proteus vulgaris* and *Shigella flexneri* were used and among the fungal strains *Aspergillus niger*, *Aspergillus flavus*, *Aspergillus fumigatus*, *Candida albicans*, *Mucor oryzae* and *Rhizopus indicus* were used.

ANTIBACTERIAL ACTIVITY OF SILVER NANOPARTICLES

The antibacterial activity of the AgNPs was tested at 10µg concentration. The results were assessed on the basis of zone of inhibition. Based on the optimization of AgNP synthesis, it was decided to analyze the AgNPs synthesized only by exposure to sunlight for 20 minutes. Chloramphenicol was used as the standard antibiotic.

DETERMINATION OF ANTIBACTERIAL ACTIVITY OF AgNPs BY AGAR WELL DIFFUSION METHOD

The AgNPs were evaluated for their antibacterial activity against above mentioned bacterial strains. All assays were done in duplicates, the diameter of zone of inhibition was measured in mm.

The results obtained for antibacterial activity of AgNPs by agar well diffusion method are presented in **TABLE 1** and **PLATE 3.** The AgNPs was found to be more effective against *Proteus vulgaris, Escherichia coli, Pseudomonas aeruginosa, Staphylococcus aureus* and *Salmonella typhi.* It was moderately effective against, *Klebsiella pneumoniae* and *Shigella flexneri.*

Several studies have been reported in the literature indicating the antibacterial activity of AgNPs. Antimicrobial property of silver nanoparticles synthesized by chemical method has also been studied by Huang *et al.* (2010). They reported that silver nanoparticles in size range 10–25 nm are effective antimicrobial agents. Moreover, Shrivastava *et al.* (2007) studied the interaction stage between Ag nanoparticles and bacteria (*E. coli*). They found that at initial stage of the interaction Ag nanoparticles adhere to bacterial cell wall subsequently penetrate the bacteria and kill bacterial cell by destroying cell membrane.

Antimicrobial activity of biosynthesized silver nanoparticles against both Gram-negative (*E. coli*) and Gram-positive (*S. aureus*) microorganisms at different concentrations showed that they revealed a strong dose-dependent antimicrobial activity against both of the test microorganisms. The concentration of biosynthesized nanoparticles were increased with decrease in the microbial growth. Biosynthesized silver nanoparticles were observed to exhibit more antimicrobial activity on Gram-negative microorganism than Gram-positive ones (Singhal *et al.*, 2011).

TABLE 1

ANTIBACTERIAL ACTIVITY OF AgNPs BY AGAR WELL DIFFUSION METHOD

MICROORGANISMS	Diameter of zone of inhibition in mm	
	AgNPs	CONTROL (Chloramphenicol)
Proteus vulgaris	10	15
Escherichia coli	12	21
Staphylococcus aureus	12	19
Salmonella typhi	11	15
Pseudomonas aeruginosa	6.0	10
Klebsiella pneumonia	5.0	15
Shigella flexneri	3.0	10

PLATE 4

ANTIBACTERIAL ACTIVITY OF AgNPs

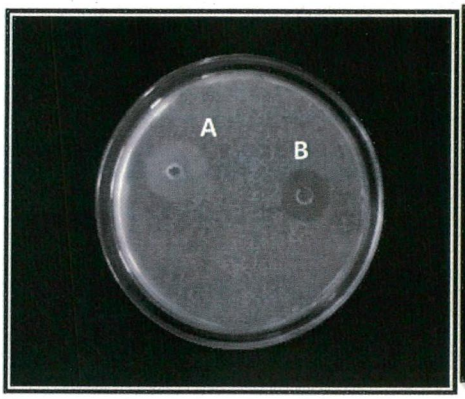

Salmonella typhi

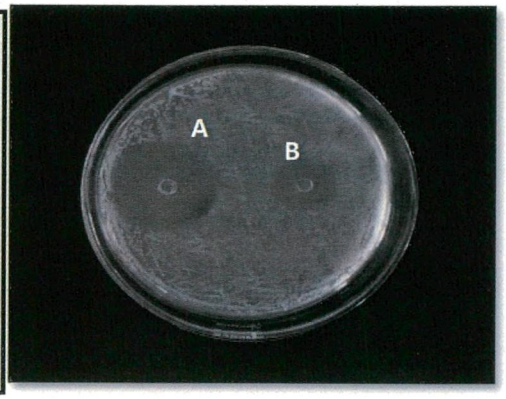

Staphylococcus aureus

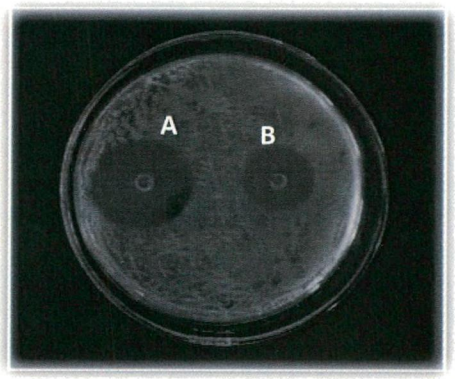

Escherichia coli

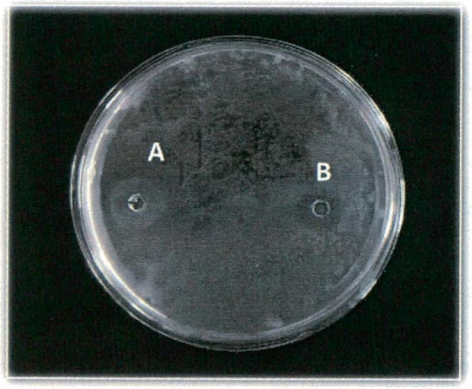

Pseudomonas aeruginosa

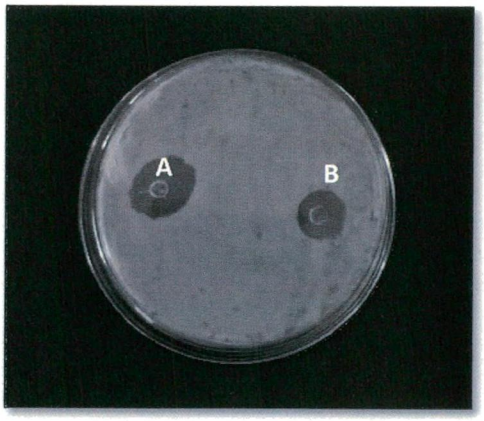

Proteus vulgaris

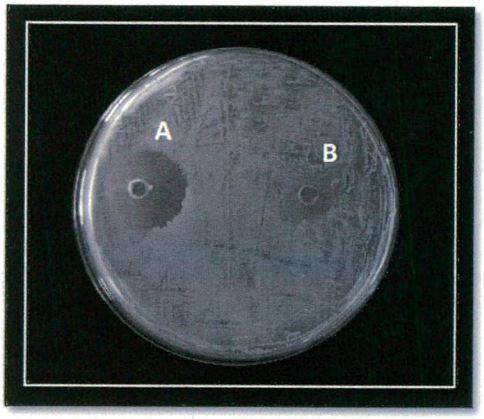

Klebsiella pneumonia

A – Control **B - AgNPs**

Green synthesis of silver nanoparticles of *Psidium guajava* showed very strong inhibitory effects against *S. aureus* (Sriram and pandidurai, 2014).

Augustine *et al.* (2013) demonstrated that silver nanoparticles synthesized at all the silver nitrate concentrations displayed antibacterial activity against both *E. coli* and *S. aureus*. Nanoparticles prepared using 1 mM silver nitrate was the most efficient to inhibit both *E. coli* and *S. aureus*. There is a decrease in antibacterial activity as the concentration of silver nitrate increased.

Antibacterial activity of silver nanoparticles was found to be dependent on the size of silver particles and as the size increases the antibacterial activity decreases (Panáček *et al.*, 2006). All the synthesized nanoparticles have shown more antibacterial activity against *S. aureus* than *E. coli* (Sadeghi *et al.*, 2010; Shrivastava *et al.*, 2007), probably due to the difference in cell walls between Gram-positive and Gram-negative bacteria. Karsha and Lakshmi, (2010) reported the antibacterial activity of black pepper (*P. nigrum* Linn.) and its mode of action on both Gram-negative and Gram-positive bacteria.

With these reports, our study indicates that the AgNPs showed good antibacterial activity against *Pseudomonas aeruginosa*, *Proteus vulgaris*, *Escherichia coli*, *Staphylococcus aureus* and *Salmonella typhi*.

ANTIFUNGAL ACTIVITY OF SILVER NANOPARTICLES

AGAR PLUG METHOD

The antifungal assay was performed for the silver nanoparticles. The zone of inhibition was determined and the results obtained are presented in **TABLE 2** and **PLATE 4**.

The results of agar plug method indicated that the antifungal activity of AgNPs showed 100% activity against *Aspergillus niger, Aspergillus flavus* and *Candida albicans.* It exhibited more than 50% inhibition against *Rhizopus indicus, Aspergillus fumigatus* and *Mucor oryzae*. Our results indicated that AgNPs showed better antifungal activity against *Candida albicans, Aspergillus niger and Aspergillus flavus*.

TABLE 2

ANTIFUNGAL ACTIVITY OF AgNPs BY AGAR PLUG METHOD

MICROORGANISMS	GROWTH INHIBITION	
	AgNPs	CONTROL (Nystatin)
Aspergillus niger	+++	+++
Aspergillus fumigates	++	+++
Aspergillus flavus	+++	+++
Rhizopus indicus	++	+++
Mucor oryzae	++	+++
Candida albicans	+++	+++

+++ 100% inhibition, ++ ≤ 50% inhibition, + ≥ 50%, - - no inhibition

Samuel and Guggenbichler, (2004) suggested that the nanoparticles efficiently penetrate microbial cells, that lower concentrations of nanosized silver particles would be sufficient for microbial control. This approach could be more efficient than existing treatments, especially for certain organisms that are less sensitive to antibiotics because of their resistance to cell penetration.

Woo *et al.* (2009) evaluated the antifungal activity of silver nanoparticles against the fungal phytopathogen *Raffaelea sp.* The activity demonstrated that the nanoparticles strongly inhibited fungal development and growth and damaged cell walls.

Vivek *et al.* (2011) reported that the evaluation of antibiotic resistant pathogenic fungi has stimulated the search for effective antifungal agent from alternative sources. The silver nanoparticles synthesized from *Gelidiella acerosa* seem to be promising and effective antifungal agent against the fungal strains.

PLATE 5

ANTIFUNGAL ACTIVITY OF AgNPs

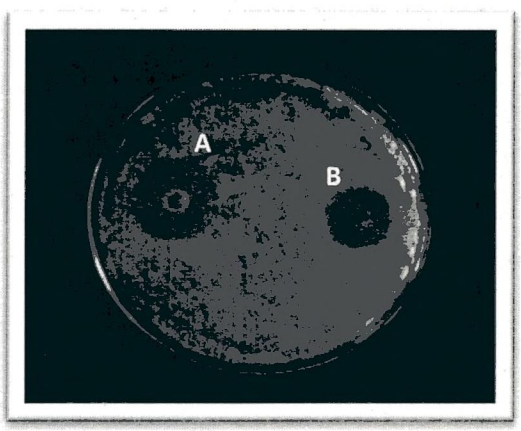

Candida albicans

Aspergillus flavus

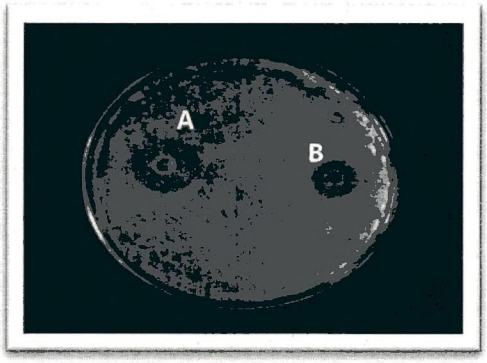

Mucor oryzae

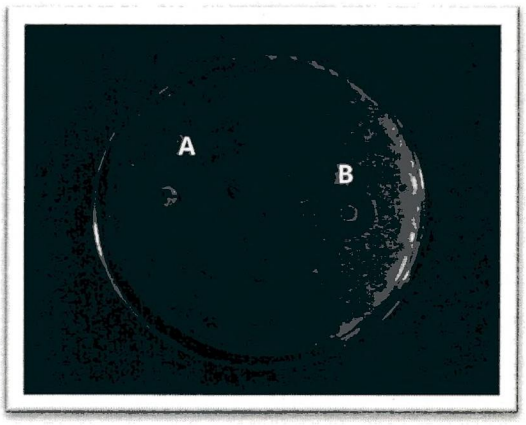

Rhizopus indicus

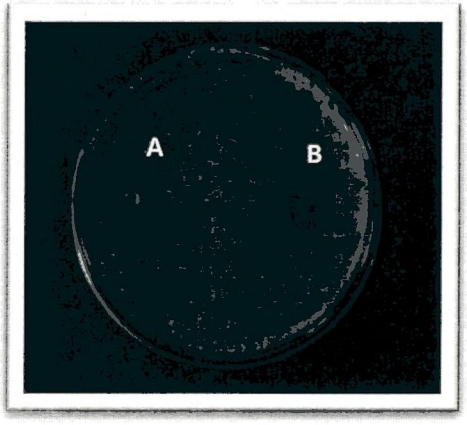

Aspergillus niger

A – Control ***B* - AgNPs**

The biosynthesized silver nanoparticles from *E. chapmaniana* showed excellent antimicrobial activity. The silver nanoparticles showed good inhibition activity towards *C. albicans* (Sulaiman *et al.*, 2013).

IN SILICO APPROACHES

In silico screening of the ligand and/or of the receptors has become an essential tool to facilitate the drug discovery process but compound collections are needed to carry out such *in silico* experiments. In the modern drug designing, molecular docking is used for understanding the information of drug receptor interactions and is frequently used to predict the binding orientation of small molecule drug candidates to their protein targets in order to predict the affinity and activity of the small molecule (Onkara *et al.*, 2013).

The component eupalitin, a flavanoid isolated from *A. adenophora* was subjected to *in silico* studies for their efficacy against the target protein dihydrofolate reductase of the most different susceptible organisms namely the bacterial strains *Escherichia coli, Staphylococcus aureus* and *Bacillus anthracis* and the fungal strain of *Candida albicans* and *Candida glabrata.* The target proteins selected were 4PSS for *Escherichia coli*, 3F0Q for *Staphylococcus aureus*, 3S9U for *Bacillus anthracis*, 4HOG for *Candida glabrata* and 4HOE for *Candida albicans*. The 3D structures of the target proteins were obtained from the Protein Data Bank and the structures were refined using the protein preparation wizard module. The molecular docking and ADME studies were performed to characterize the active components.

ADME STUDIES

The ligands with good pharmacological and druggish properties are very crucial for structure based drug discovery. The ADMET (absorption, distribution, metabolism, excretion and toxicity) is the most important part of pharmacological studies of lead molecules and these can be predicted by computational biology tools (Bora *et al.*, 2011). To be an effective drug, a compound not only must be active against a target, but also possess the appropriate ADME profile necessary to make it suitable for use as a drug. QikProp 4.0 module of Schrodinger predicts physically significant descriptors and pharmaceutically relevant properties of organic molecules. The QikProp results of the ligand, eupalitin is given in **TABLE 3**.

TABLE 3

ADME RESULTS OF LIGAND USING QikProp

S.No	DESCRIPTORS	STANDARD VALUES	LIGAND VALUE (EUPALITIN)
1	Molecular weight (Da)	130.0-725.0	330.29
2	Number of hydrogen bond donors	0.0/6.0	2
3	Number of hydrogen bond acceptors	2.0-20.0	5.25
4	Qp log P for octanol/water	-2.0/6.5	2.1
5	Apparent CaCo-2 permeability (nm/sec)	<25 poor, >500 great	211
6	Apparent MDCK permeability (nm/sec)	<25 poor, >500 great	92
7	Lipinski rule of 5 violation	(maximum is 4)	0
8	% Human oral Absorption in GI (± 20%)	(<25% is poor)	80.9%
9	Qualitative model for human oral absorption	(> 80% is high)	High

The QikProp results for eupalitin showed that the compound does not violate the Lipinski's rule of five, which is a refinement of drug likeness and is used to predict whether a chemical compound will have pharmacological or biological activity as an orally active drug in humans. The percentage of human oral absorption in gastrointestinal tract is high for eupalitin.

Number of hydrogen bond donors and acceptors were found to be 2 and 5.25 respectively. The lipophilicity is expressed as the partition co-efficient P in octanol/water. Eupalitin is found to be lipophilic, indicating good absorption and distribution. Therefore the compound eupalitin possesses good pharmacological activity, was then subjected to docking using glide.

MOLECULAR DOCKING USING GLIDE

The ligand eupalitin was docked to the target proteins using Glide in standard precision mode. A correlation was calculated by Glide score. For the prediction of results mainly four parameters are considered namely G-score, Glide energy, H-bonds and Good contacts, which indicates the binding affinity of ligand towards receptor.

Staphylococcus aureus

Dihydrofolate reductase protein (3F0Q) in *staphylococcus aureus* was docked with eupalitin. The affinity of eupalitin with the target protein 3F0Q and the top ranked poses generated by Glide SP docking are given in **TABLE 4**. The docking efficiency and the molecular interactions showing good contacts of eupalitin with 3F0Q are depicted in **FIGURES 5** and **6** respectively.

TABLE 4

GLIDE SP DOCKING OF THE LIGAND WITH THE TARGET PROTEINS 3F0Q OF *Staphylococcus aureus*

	Target proteins	**Glide score**	**Energy (kcal/mol)**	**Good contacts**	**Pose number**	**Number of H- bonds**
EUPALITIN	3F0Q	-5.883	-30.2	272	29	1

Table 7 shows that eupalitin showed good glide score of -6.199 with target 3F0Q. The ligand also possessed a good minimum energy of -30.2. Eupalitin showed greater interaction with the target protein 3F0Q through two H-bonds. Eupalitin showed more good contacts with 3F0Q protein. The ligand was found to possess good docking efficiency with the target protein 3F0Q, revealing their importance to influence the activity of protein.

Escherichia coli

The affinity of eupalitin with the dihydrofolate reductase protein of *E. coli* is 4PSS and the top ranked poses generated by Glide SP docking are given in **TABLE 5**. The docking efficiency and the molecular interactions showing good contacts of eupalitin with 4PSS are depicted in **FIGURES 7** and **8**.

TABLE 5

GLIDE SP DOCKING OF THE LIGAND WITH THE TARGET PROTEIN 4PSS OF *Escherichia coli*

	Target proteins	**Glide score**	**Energy (kcal/mol)**	**Good contacts**	**Pose number**	**Number of H- bonds**
EUPALITIN	4PSS	-6.903	-43.02	296	47	1

Eupalitin showed good interaction with 4PSS through one H-bond and showed good glide score of -6.903. The ligand also possessed a good minimum energy of -43.02. Eupalitin showed very good contacts with 4PSS protein. The ligand was found to possess good docking efficiency with the target protein 4PSS.

Bacillus anthracis

The target protein (3S9U) in *Bacillus anthracis* was docked with eupalitin. The affinity of eupalitin with the target protein 3S9U and the top ranked poses generated by Glide SP docking are given in **TABLE 6**. The docking efficiency and the molecular interactions showing good contacts of eupalitin with 3S9U are depicted in **FIGURES 9** and **10** respectively.

TABLE 6

GLIDE SP DOCKING OF THE LIGAND WITH THE TARGET PROTEINS 3S9U OF *Bacillus anthracis*

EUPALITIN	**Target proteins**	**Glide score**	**Energy (kcal/mol)**	**Good contacts**	**Pose number**	**Number of H- bonds**
	3S9U	-6.199	-38.4	197	177	4

The target protein (3S9U) also possessed a good minimum energy of -38.4. The top ranked poses generated by Glide SP docking between the ligand and target protein of 3S9U is 177. Eupalitin showed good interaction with the target protein 3S9U through four H- bond.

Candida albicans

The target protein in *Candida albicans* 4HOE was docked with eupalitin. The affinity of eupalitin with the target protein 4HOE and the top ranked poses generated by Glide SP docking are given in **TABLE 7**. The docking efficiency and the molecular interactions showing good contacts of eupalitin with 4HOE are depicted in **FIGURES 11** and **12** respectively.

TABLE 7

GLIDE SP DOCKING OF THE LIGAND WITH THE TARGET PROTEINS 4HOE OF *Candida albicans*

EUPALITIN	**Target proteins**	**Glide score**	**Energy (kcal/mol)**	**Good contacts**	**Pose number**	**Number of H- bonds**
	4HOE	-5.54	-36.5	247	161	1

Eupalitin showed good interaction with the target protein 4HOE through one H-bond. Glide score, pose number, energy and good contacts of eupalitin with the target protein 4HOE were -5.54, 161, -36.5 and 247 respectively.

Candida glabrata

The target protein in *Candida glabrata* 4HOG was docked with eupalitin. The affinity of eupalitin with the target protein 4HOG and the top ranked poses generated by Glide SP docking are given in **TABLE 8**. The docking efficiency and the molecular interactions showing good contacts of eupalitin with 4HOG are depicted in **FIGURES 13** and **14** respectively.

TABLE 8

GLIDE SP DOCKING OF THE LIGAND WITH THE TARGET PROTEINS 4HOG OF *Candida glabarata*

	Target proteins	Glide score	Energy (kcal/mol)	Good contacts	Pose number	Number of H- bonds
EUPALITIN	4HOG	-4.75	-34.5	143	218	3

From the table 8, it was evident that eupalitin had showed good glide score of -4.75 with target 4HOG. The ligand also possessed a good minimum energy of -34.5. Eupalitin showed greater interaction with the target protein 4HOG through three H-bonds. Eupalitin showed more good contacts with 4HOG protein. The ligand was found to possess good docking efficiency with the target protein 4HOG, revealing their importance to influence the activity of protein.

Drug discovery is a time consuming, expensive and interdisciplinary process whereas advances in computational techniques and hardware solutions have enabled *in silico* methods to speed up lead optimization and identification (Rao and Srinivas, 2011).

ADME screening was carried out in order to understand the pharmacokinetic behavior of reported derivatives using descriptors like Human Intestinal Absorption (HIA), Lipinski rule of five, Blood brain barrier penetration, Hepato toxicity, Aqueous solubility and Inhibition probabilities (Rochani *et al.*, 2010).

Molecular docking was to form favorable interactions with the plant derived quercetin into the active site of human inducible nitric oxide synthase (Singh and Konwar, 2012).

Poshiya and Patel, (2011) has screened to analyse the molecular docking simulations on 4-methyl-2-oxo-2H-chromen-7-yl benzoate analogues as probable candidates for inhibiting DNA gyrase subunit-B of *Staphylococcus aureus*. Molecular docking was carried out for total eight

FIGURE 5

DOCKING OF EUPALITIN WITH THE TARGET PROTEINS 3F0Q OF *Staphylococcus aureus*

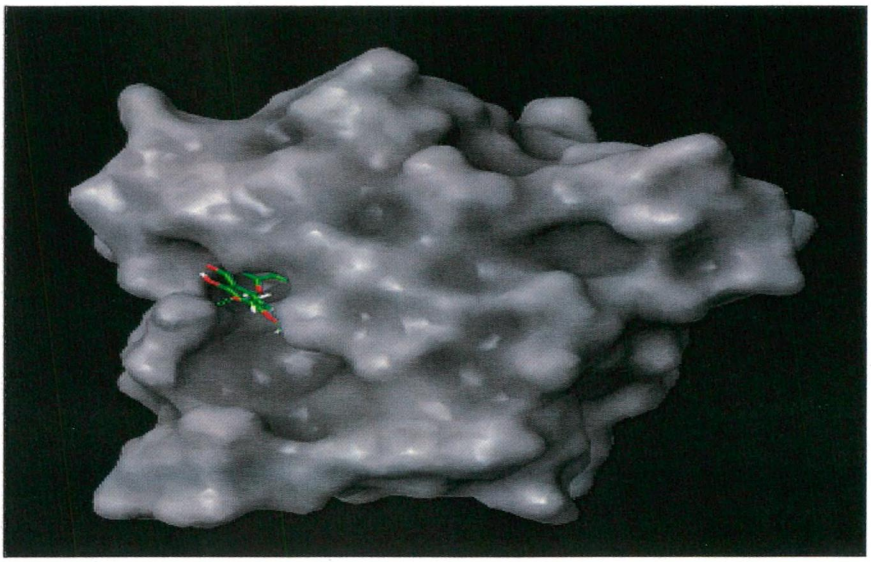

FIGURE 6

MOLECULAR INTERACTION OF EUPALITIN WITH THE TARGET PROTEIN 3F0Q *Staphylococcus aureus*

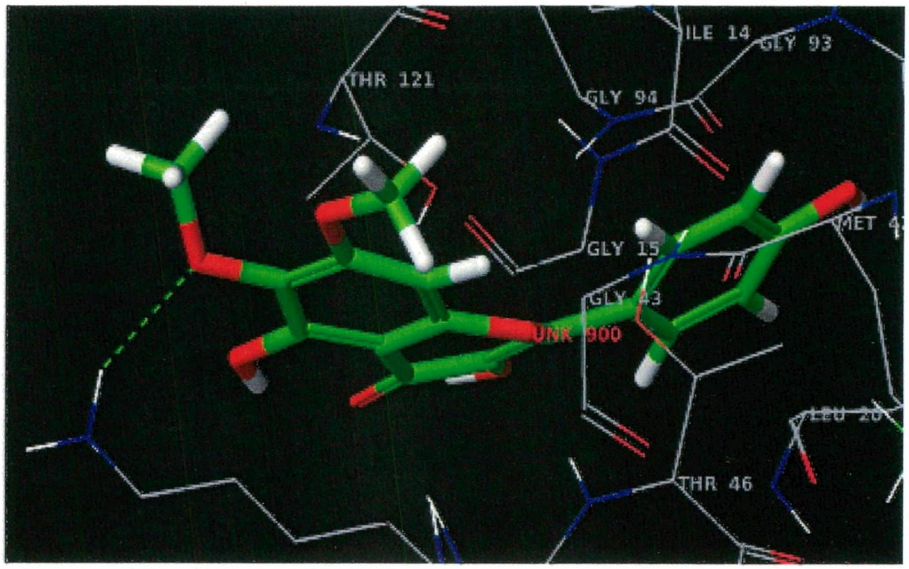

FIGURE 7

DOCKING OF EUPALITIN WITH THE TARGET PROTEIN 4PSS OF *Escherichia coli*

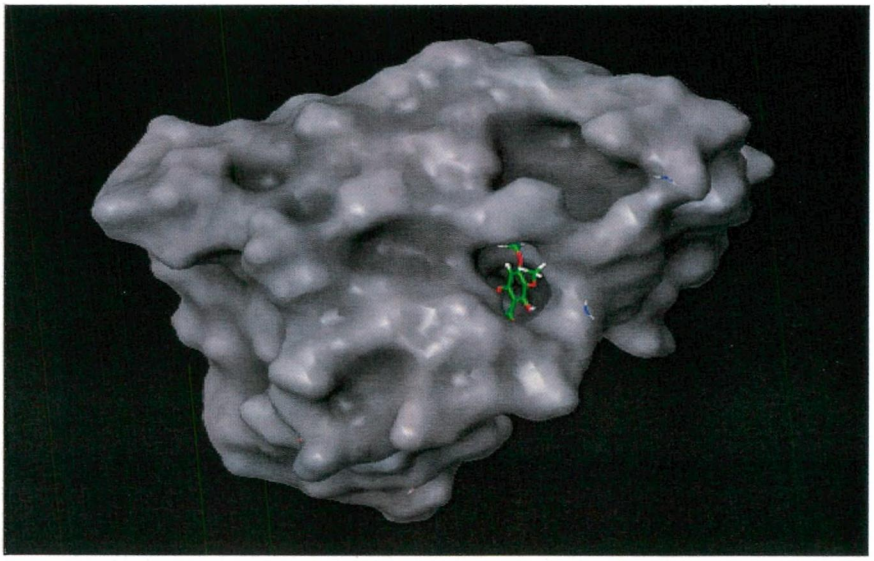

FIGURE 8

MOLECULAR INTERACTION OF EUPALITIN WITH THE TARGET PROTEIN 4PSS OF *Escherichia coli*

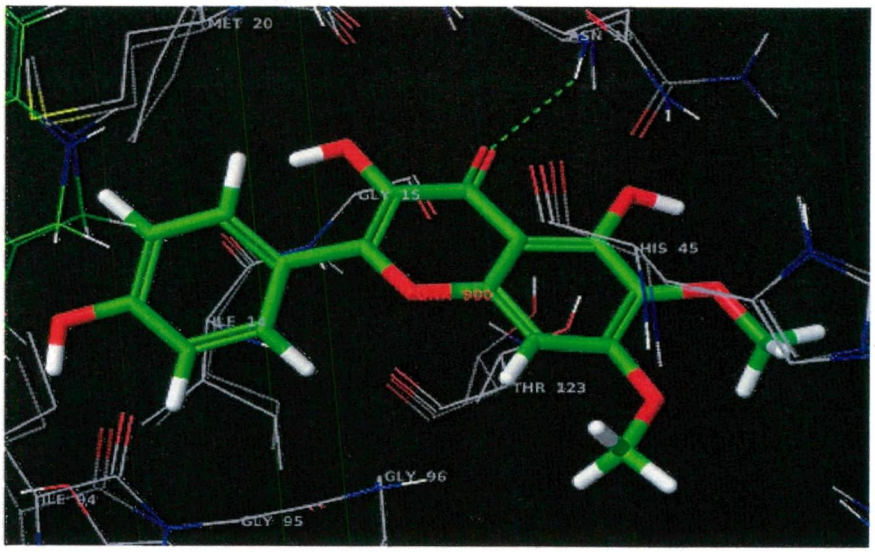

FIGURE 9

DOCKING OF EUPALITIN WITH THE TARGET PROTEIN 3S9U OF *Bacillus anthracis*

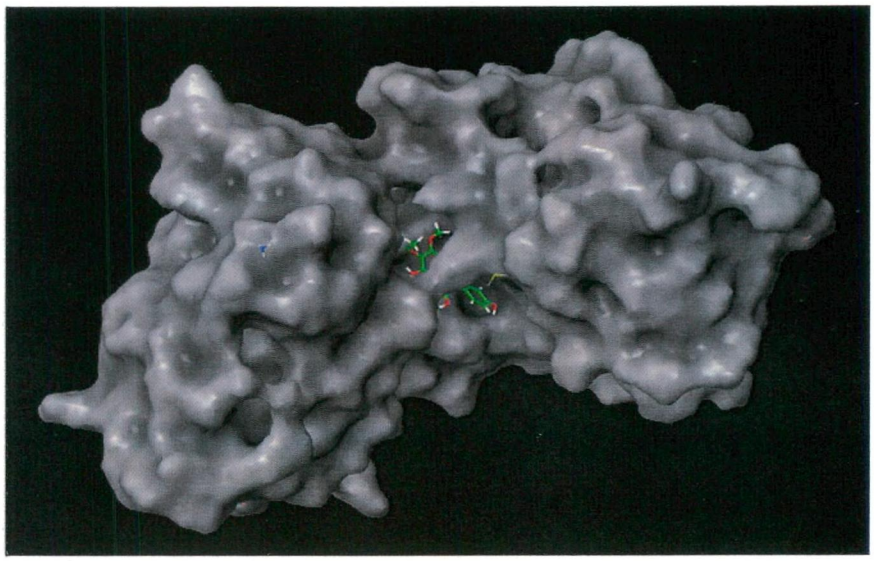

FIGURE 10

MOLECULAR INTERACTION OF EUPALITIN WITH THE TARGET PROTEIN 3S9U OF *Bacillus anthracis*

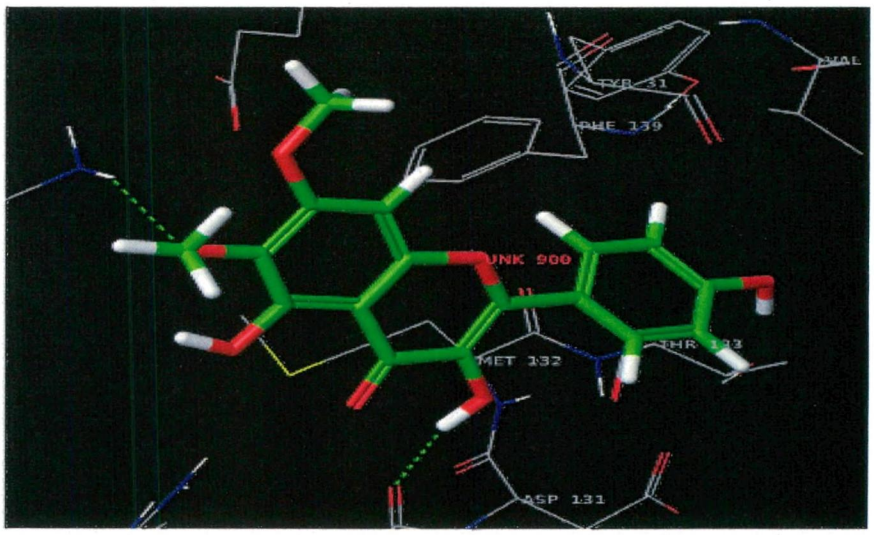

FIGURE 11

DOCKING OF EUPALITIN WITH THE TARGET PROTEIN 4HOE OF *Candida albicans*

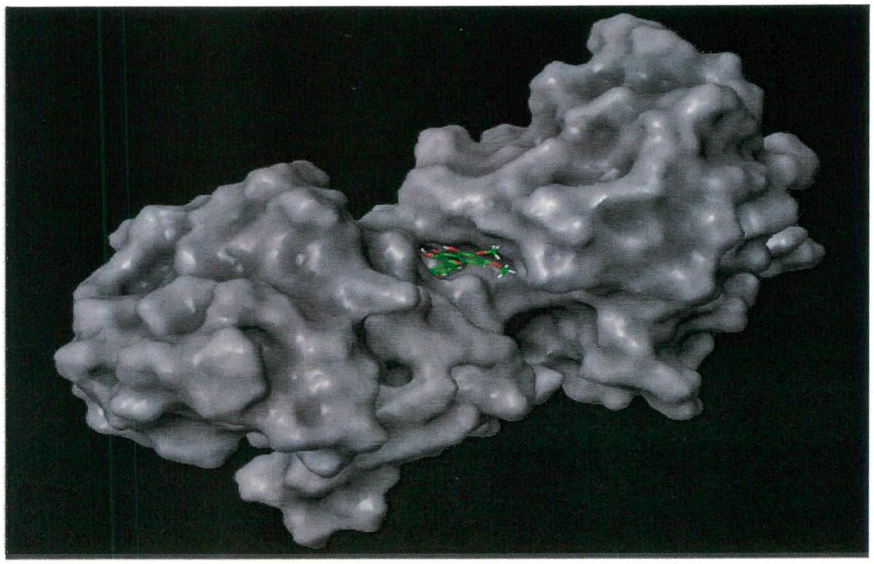

FIGURE 12

MOLECULAR INTERACTION OF EUPALITIN WITH THE TARGET PROTEIN 4HOE OF *Candida albicans*

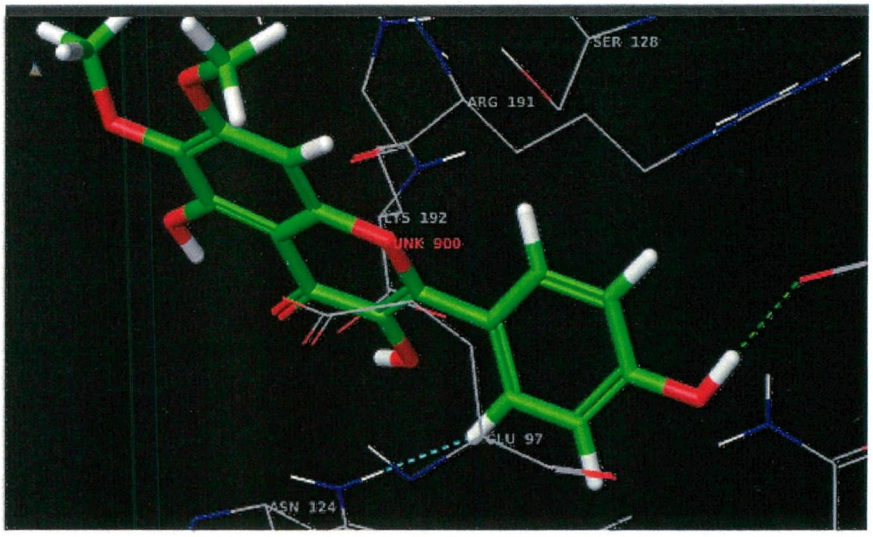

FIGURE 13

DOCKING OF EUPALITIN WITH THE TARGET PROTEIN 4HOG OF *Candida glabarata*

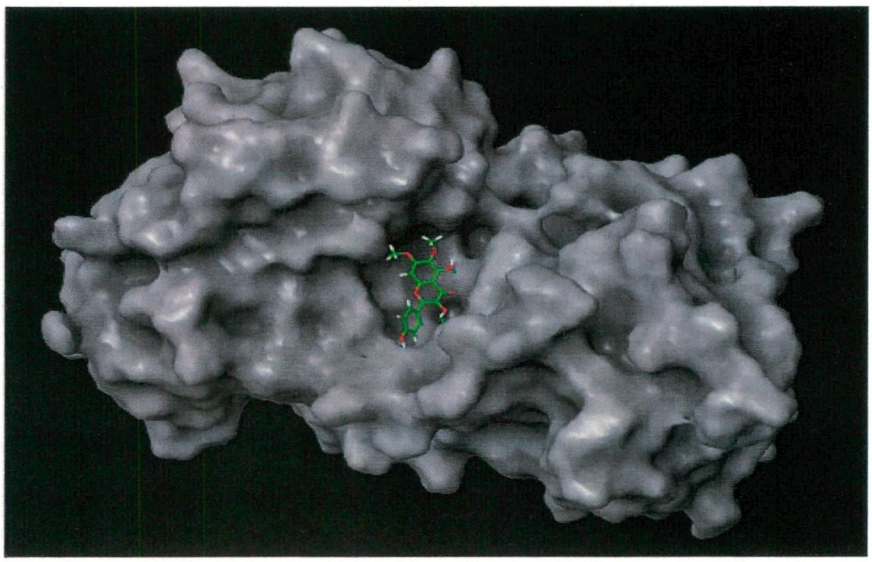

FIGURE 14

MOLECULAR INTERACTION OF EUPALITIN WITH THE TARGET PROTEIN 4HOG OF *Candida glabarata*

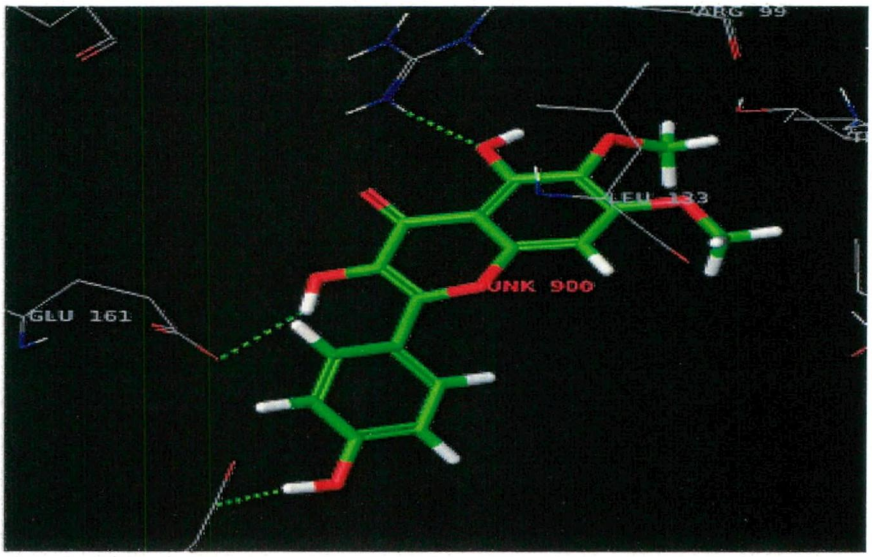

derivatives of 4-methyl-2-oxo-2H-chromen-7-yl benzoate. Among them CHR-7 and CHR-8 showed the better binding interactions within active site of DNA-gyrase B subunit

Plant derived compounds such as baicalein, biochanin, carnosol, genistein, orobol, resveratrol, rhein, gallic acid, pyrithione, resveratrol and linozolid for potential activity against a lethal factor in *Staphylococcus aureus*. The compound orobol was found to interact more towards the target protein showing highest docking score (Hariprasath, 2011).

Also, it is clearly evident that from our *in silico* studies, eupalitin has a good bioavailability, a non-toxic compound which can be developed into a drug. The docking results of eupalitin with the target protein dihydrofolate reductase of different microorganisms indicated that eupalitin will easily inhibit the microbes that are responsible for several diseases.

Thus, the present study strongly reveals the medicinal value of the compound of plant origin, eupalitin and scientifically validates it for use as a novel drug candidate for antimicrobial activity.

The present findings of this study are summarized and presented with the conclusions drawn, in the following chapter.